



Sharif University of Technology  
Scientia Iranica  
Transactions F: Nanotechnology  
<http://scientiairanica.sharif.edu>



# Isogeometric vibration analysis of small-scale Timoshenko beams based on the most comprehensive size-dependent theory

A. Norouzzadeh<sup>a</sup>, R. Ansari<sup>a,\*</sup>, and H. Rouhi<sup>b</sup>

a. Department of Mechanical Engineering, University of Guilan, Rasht, P.O. Box 3756, Iran.

b. Department of Engineering Science, Faculty of Technology and Engineering, East of Guilan, University of Guilan, P.O. Box 44891-63157, Rudsar-Vajargah, Iran.

Received 21 October 2017; received in revised form 29 January 2018; accepted 16 April 2018

## KEYWORDS

Nonlocal elasticity theory;  
Strain gradient elasticity theory;  
Timoshenko nanobeam.

**Abstract.** By taking the nonlocal and strain gradient effects into account, the vibrational behavior of Timoshenko micro- and nano-beams is studied in this paper based on a novel size-dependent model. The nonlocal effects are captured using both differential and integral formulations of Eringen's nonlocal elasticity theory. Moreover, the strain gradient influences are incorporated into the model according to the most general form of strain gradient theory, which can be reduced to simpler strain gradient-based theories such as modified strain gradient and modified couple stress theories. Hamilton's principle is employed to derive the variational form of governing equations. The isogeometric analysis (IGA) is then utilized for the solution approach. Comprehensive results for the effects of small-scale and nonlocal parameters on the natural frequencies of beams under various types of boundary conditions are given and discussed. It is revealed that using the differential nonlocal strain gradient model for computing the fundamental frequency of cantilevers leads to paradoxical results, and one must recourse to the integral nonlocal strain gradient model to obtain consistent results.

© 2018 Sharif University of Technology. All rights reserved.

## 1. Introduction

The vibrational analysis of small-scale beam-type structures is of great importance due to the related applications, especially in micro- and nano-electromechanical systems (MEMS and NEMS). Among theoretical approaches used to study the mechanical behaviors of micro- and nano-beams, continuum models based upon the Euler-Bernoulli, Timoshenko, and other beam theories are extensively used. However, the classical continuum models have not the

capability of considering small-scale effects. The reason can be found in the local nature of classical elasticity and the lack of length scale parameters in such theories. Therefore, some non-classical or size-dependent elasticity theories have been developed. There are many research efforts which confirm the necessity of using generalized continuum models (e.g., [1-5]).

The nonlocality is an important small-scale influence on the mechanics of nanostructures. According to the nonlocal elasticity theory, the stress tensor at a reference point in the body depends not only on the strain tensor at that point, but also on the strain tensor at all other points of the body. This theory was first developed by Kröner [6], Krumhansl [7], and Kunin [8]. Moreover, its first formal introduction was related to the papers of Eringen [9] and Eringen and Edelen [10].

\*. Corresponding author. Tel./Fax: +98 13 33690276  
E-mail address: [r\\_ansari@guilan.ac.ir](mailto:r_ansari@guilan.ac.ir) (R. Ansari)

Based on the original version of nonlocal theory, which is in the integral form, kernel functions are used so as to consider the nonlocal effects. In 1983, Eringen [11] formulated the differential form of the theory by Green function of linear differential operator as the kernel function. Since working with the resulting differential equations is simpler than working with integro-partial differential equations derived from the integral form of the theory, the differential form of nonlocal elasticity theory is extensively employed by researchers. Refs. [12-19,20-26,27-32] can be mentioned as examples of the differential nonlocal model applied to the problems of nanoplates, nanobeams, and nanoshells, respectively. In this regard, Norouzzadeh and Ansari [19] employed the nonlocal continuum along with surface elasticity theory to present a size-dependent analysis of the vibration characteristics of low-dimensional rectangular and circular plates. Sedighi et al. [25] utilized the Euler-Bernoulli beam model to investigate the stability of NEMS with the consideration of conductivity, surface energy, and nonlocal effects. Also, Civalek and Demir [26] proposed a simple nonlocal beam element to capture the size impacts on the buckling behavior of protein microtubules.

However, using the differential nonlocal model in some problems may lead to paradoxical results, and recourse must be made to the original (integral) form of the nonlocal theory. A well-known paradox occurs when this model is used for computing fundamental frequencies and deflections of beams under clamped-free boundary conditions. It is generally accepted that increasing the nonlocal parameter has a decreasing effect on the stiffness of structure. But, the first natural frequency and deflection of cantilevers respectively increases and decreases as the nonlocal parameter gets larger. Therefore, capturing the nonlocal effects within the framework of integral form of nonlocal elasticity has recently attracted the attention of several research workers [33-39].

The Strain Gradient Theory (SGT) is another non-classical continuum theory to consider the size-dependent behavior of small-scale structures through using length scale parameters. The most general form of SGT was proposed by Mindlin [40,41]. Based upon first- and second-order Mindlin's SGT, the first and second derivatives of the strain tensor effective on the strain energy density are taken into account, respectively. In the constitutive relations of first-order SGT, there are five material length scale parameters (in addition to the classical material constants) to characterize the size-dependent behavior of structure. There are also some simplified forms of SGT such as the modified SGT of Lam et al. [42], SGT of Aifantis [43], and modified couple stress theory of Yang et al. [44]. Tracing the development of literature in this

area demonstrates the contribution of many researchers in recent years, e.g. [45-57]. Among them, Chen and Li [47] proposed the composite laminated Timoshenko beam model on the basis of modified couple stress theory and anisotropic constitutive equations. Also, by considering thermal and mechanical loadings, Sadeghi et al. [51] studied the thick-walled Functionally Graded (FG) small-scale cylinders using the strain gradient elasticity. Tadi Beni [54] developed the size-dependent geometrically nonlinear formulation of FG piezoelectric beams and detected the responses of bending, buckling, and free vibration problems of such structures. To do so, he used the consistent model of couple stress theory proposed by Hadjesfandiari and Dargush [58].

Recently, simultaneous capture of nonlocal and strain gradient effects by a unified model, called the nonlocal strain gradient model, has attracted much attention. According to the nonlocal strain gradient theory, the stress tensor at a reference point in the body depends on the strain and strain gradient tensors at all points of the body. In this regard, Narendar and Gopalakrishnan [59] developed nonlocal strain gradient models. They studied the ultrasonic wave propagation of nano-rods by taking the nonlocality and strain gradient effects into account simultaneously. Some other researchers developed nonlocal strain gradient models to address various problems of small-scale structures. The reader is referred to [60-65] as some recently published papers on this issue.

In the present paper, a novel nonlocal strain gradient model is developed to study the free vibrations of small-scale beams. To consider the nonlocal effect, both differential and integral forms of Eringen's nonlocal theory are applied. In addition, the strain gradient influences are incorporated into the model based on the most general form of strain gradient formulation [40], which encompasses the modified strain gradient and couple stress theories (MSGT and MCST). The beam is also modeled according to the Timoshenko beam theory accounting for shear deformation effect. First, the variational formulations are obtained for integral nonlocal strain gradient and differential nonlocal strain gradient models using Hamilton's principle. Apart from the novelty of work in its formulation (general form of nonlocal elasticity in conjunction with the most general form of SGT), the solution approach is another novel aspect of the current research; the obtained governing equations are solved through an isogeometric analysis (IGA). IGA [66,67] is a powerful numerical method whose sources of inspiration are the Finite Element Method (FEM) and the Computer Aided Design (CAD). Construction of exact geometry via Non-Uniform Rational B-Splines (NURBS) and easy implementation of geometry refinement tools are the main advantages of IGA. Finally, comprehensive numerical results are presented in order to investigate

the strain gradient/nonlocal effects on the vibrations of beams subject to different end conditions.

## 2. Derivation of variational formulation

### 2.1. Integral nonlocal strain gradient model

To take the strain gradient effects into account, SGT according to [40] is employed. By considering the following relations:

$$s_{ij} = \frac{\partial \bar{w}}{\partial e_{ij}}, \quad t_{ijk} = \frac{\partial \bar{w}}{\partial \zeta_{ijk}}, \quad (1)$$

and the classical stress tensor as:

$$s_{ij}(x) = \lambda \delta_{ij} e_{kk}(x) + 2\mu e_{ij}(x) = A_{ijkl} e_{kl}(x), \quad (2)$$

the components of double stress tensors  $t_{ijk}$  can be obtained through the following formula:

$$\begin{aligned} t_{ijk}(x) &= \frac{1}{2} a_1 (\delta_{ij} \zeta_{kl}(x) + 2\delta_{jk} \zeta_{li}(x) + \delta_{ik} \zeta_{jl}(x)) \\ &\quad + 2a_2 \delta_{jk} \zeta_{il}(x) + a_3 (\delta_{ij} \zeta_{lk}(x) + \delta_{ik} \zeta_{lj}(x)) \\ &\quad + 2a_4 \zeta_{ijk}(x) + a_5 (\zeta_{jki}(x) + \zeta_{kji}(x)) \\ &= \hat{A}_{ijklmn} \zeta_{lmn}(x), \end{aligned} \quad (3)$$

where  $\bar{w}$  is the strain energy density. Also,  $e_{ij}$  and  $\zeta_{ijk}$  denote the strain and second-order deformation gradient tensors, respectively. The classical elastic tensor,  $A_{ijkl}$ , includes classical Lamé's parameters given by:

$$\lambda = \frac{E\nu}{1-\nu^2}, \quad \mu = \frac{E}{2(1+\nu)}, \quad (4)$$

in which  $E$  and  $\nu$  stand for Young's modulus and Poisson's ratio, respectively.

In addition to classical Lamé's parameters, the sixth-order  $\hat{A}_{ijklmn}$  elastic tensor contains five non-classical constants ( $a_1, a_2, \dots, a_5$ ), which are used to capture the size effects. The theory used herein is the most general form of SGT with the capability of being reduced to other simplified theories. For instance, the modified strain gradient model of Lam et al. [42] can be retrieved by the following relations:

$$\begin{aligned} a_1 &= \mu \left( l_0^2 - \frac{4}{15} l_1^2 \right), \quad a_2 = \mu \left( l_0^2 - \frac{1}{15} l_1^2 - \frac{1}{2} l_2^2 \right), \\ a_3 &= -\mu \left( \frac{4}{15} l_1^2 + \frac{1}{2} l_2^2 \right), \quad a_4 = \mu \left( \frac{1}{3} l_1^2 + l_2^2 \right), \\ a_5 &= \mu \left( \frac{2}{3} l_1^2 - l_2^2 \right). \end{aligned} \quad (5)$$

Moreover, the present model can be reduced to the

modified couple stress model of Yang et al. [44] via these substitutions:

$$a_1 = a_4 = -2a_2 = -2a_3 = -a_5 = \mu l^2, \quad (6)$$

or the strain gradient model proposed by Aifantis [43] is obtained through:

$$a_1 = a_3 = a_5 = 0, \quad a_2 = \frac{1}{2} \lambda l^2, \quad a_4 = \mu l^2, \quad (7)$$

where  $l_0$ ,  $l_1$ , and  $sl_2$  (or  $l$ ) are material length scale parameters, which can be determined based on experimental tests. As a well-known example, Lam et al. [42] presented an investigation into the strain gradient behavior of micro-scale beams. Park and Gao [68] deduced that by considering the results of Lam et al. [42] in case of  $l_0 = l_1 = l_2 = l$  and isotropic epoxy material properties, the length scale parameter can be determined as  $l = 17.6 \mu\text{m}$ .

Now, the formulation of nonlocal elasticity is introduced. The constitutive relations based upon the original integral form of Eringen's nonlocal theory [9,10] for a 1D structure are expressed as:

$$\begin{aligned} S_{ij}(\bar{x}) &= \int_x k(|x - \bar{x}|, \kappa) s_{ij}(x) dx \\ &= \int_x k(|x - \bar{x}|, \kappa) A_{ijkl} e_{kl}(x) dx, \end{aligned} \quad (8)$$

$$\begin{aligned} T_{ijk}(\bar{x}) &= \int_x k(|x - \bar{x}|, \kappa) t_{ijk}(x) dx \\ &= \int_x k(|x - \bar{x}|, \kappa) \hat{A}_{ijklmn} \zeta_{lmn}(x) dx. \end{aligned} \quad (9)$$

Here,  $S_{ij}$  and  $T_{ijk}$  are the nonlocal stress tensors of the Cauchy and double stress tensors, respectively. Based on these relations, the stress component at a reference point,  $\bar{x}$ , is obtained from the strains of all points in domain  $x$ . The nonlocality is provided using the kernel  $k$  that is a function of the neighborhood distance  $|x - \bar{x}|$  and nonlocal parameter  $\kappa = e_0 \bar{a}$ . According to [11], the ratio of internal ( $\bar{a}$ ) to external ( $\bar{l}$ ) characteristic length, i.e.  $\bar{a}/\bar{l}$ , and material constant ( $e_0$ ) are the effective parameters to determine the nonlocal stress-strain relationship. Making comparison with atomic lattice dynamics, Eringen calibrated the constant as  $e_0 \cong 0.39$  to achieve a perfect match. Also, in [12,16,27,31], Ansari et al. used the results of Molecular Dynamics (MD) simulations to propose the appropriate values of nonlocal parameter in different problems of carbon nanotubes and graphene sheets.

Now, the Timoshenko beam theory is utilized to model the beam. Based on this theory, the displace-

ment field is introduced as:

$$u_1(x, z) = u(x) + z\psi(x), \quad u_3(x, z) = w(x). \quad (10)$$

The formulation of the paper is obtained in the matrix-vector form, which is suitable to use in FEM and IGA. To this end, the following relation is given for the displacement vector:

$$\mathbf{u} = \mathbf{p}\mathbf{q}, \quad (11)$$

$$\mathbf{u}(x, z) = [u_1(x, z) \quad u_3(x, z)]^T,$$

$$\mathbf{p}(z) = \begin{bmatrix} 1 & 0 & z \\ 0 & 1 & 0 \end{bmatrix},$$

$$\mathbf{q}(x) = [u(x) \quad w(x) \quad \psi(x)]^T. \quad (12)$$

The strain and strain gradient tensors are also written as:

$$e_{ij}(x) = \frac{1}{2} \left( \frac{\partial u_i(x)}{\partial x_j} + \frac{\partial u_j(x)}{\partial x_i} \right), \quad (13)$$

$$\zeta_{ijk}(x) = (e_{jk}(x))_{,i} = \frac{1}{2} \left( \frac{\partial u_j(x)}{\partial x_k} + \frac{\partial u_k(x)}{\partial x_j} \right)_{,i} \quad (14)$$

which can be rewritten in the following vector forms:

$$\begin{aligned} \mathbf{e}(x, z) &= \begin{bmatrix} e_{xx} \\ 2e_{xz} \end{bmatrix} = \mathbf{P}_1(z) \mathbf{E}\mathbf{q}(x), \\ \boldsymbol{\zeta}(x, z) &= \begin{bmatrix} \zeta_{xxx} \\ \zeta_{zxx} \\ 2\zeta_{xxz} \end{bmatrix} = \mathbf{P}_2(z) \mathbf{H}\mathbf{q}(x), \end{aligned} \quad (15)$$

where the coefficient matrices ( $\mathbf{P}_1, \mathbf{P}_2$ ) and differentiation ones ( $\mathbf{E}, \mathbf{H}$ ) are:

$$\begin{aligned} \mathbf{P}_1(z) &= \begin{bmatrix} 1 & 0 & z \\ 0 & 1 & 0 \end{bmatrix}, \\ \mathbf{P}_2(z) &= \begin{bmatrix} 1 & 0 & z & 0 \\ 0 & 0 & 0 & 1 \\ 0 & 1 & 0 & 0 \end{bmatrix}, \\ \mathbf{E} &= \begin{bmatrix} \partial/\partial x & 0 & 0 \\ 0 & \partial/\partial x & 1 \\ 0 & 0 & \partial/\partial x \end{bmatrix}, \\ \mathbf{H} &= \begin{bmatrix} \partial^2/\partial x^2 & 0 & 0 \\ 0 & \partial^2/\partial x^2 & \partial/\partial x \\ 0 & 0 & \partial^2/\partial x^2 \\ 0 & 0 & \partial/\partial x \end{bmatrix}. \end{aligned} \quad (16)$$

From Eqs. (8) and (9), stress vectors in the reference point  $\bar{\mathbf{S}}$  and  $\bar{\mathbf{T}}$  are achieved according to the constitutive relations shown in Box I. In which  $\mathbf{A}$  and  $\hat{\mathbf{A}}$  show

the elastic matrices associated with the classical and strain gradient theories.

Hamilton's principle is used to derive the equations of motion. This principle is formulated as:

$$\delta \int_{t_1}^{t_2} (W - T) dt = 0, \quad (21)$$

where  $W$  and  $T$  denote total strain and kinetic energies, respectively.

The strain energy of the beam occupying volume  $V$  can be written as:

$$\begin{aligned} W &= \frac{1}{2} \int_V \bar{w} dV = \frac{1}{2} \int_A \int_{\bar{x}} \left( S_{ij}(\bar{x}) e_{ij}(\bar{x}) \right. \\ &\quad \left. + T_{ijk}(\bar{x}) \zeta_{ijk}(\bar{x}) \right) d\bar{x} dA, \end{aligned} \quad (22)$$

in which  $A$  is the cross section area. Consequently, the strain energy and its variation in the matrix-vector format are derived as:

$$\begin{aligned} W &= \frac{1}{2} \int_A \int_{\bar{x}} \left( \bar{\mathbf{e}}^T(\bar{x}, z) \bar{\mathbf{S}}(\bar{x}, z) \right. \\ &\quad \left. + \bar{\boldsymbol{\zeta}}^T(\bar{x}, z) \bar{\mathbf{T}}(\bar{x}, z) \right) d\bar{x} dA, \end{aligned} \quad (23)$$

$$\begin{aligned} \delta W &= \int_A \int_{\bar{x}} \left( \delta \bar{\mathbf{e}}^T(\bar{x}, z) \bar{\mathbf{S}}(\bar{x}, z) \right. \\ &\quad \left. + \delta \bar{\boldsymbol{\zeta}}^T(\bar{x}, z) \bar{\mathbf{T}}(\bar{x}, z) \right) d\bar{x} dA. \end{aligned} \quad (24)$$

The strain and strain gradient vectors at reference point ( $\bar{\mathbf{e}}, \bar{\boldsymbol{\zeta}}$ ) and corresponding variations are also presented as:

$$\begin{aligned} \bar{\mathbf{e}}(\bar{x}, z) &= \begin{bmatrix} e_{xx}(\bar{x}, z) \\ 2e_{xz}(\bar{x}, z) \end{bmatrix} = \mathbf{P}_1(z) \bar{\mathbf{E}}\bar{\mathbf{q}}(\bar{x}), \\ \delta \bar{\mathbf{e}}(\bar{x}, z) &= \mathbf{P}_1(z) \bar{\mathbf{E}}\delta \bar{\mathbf{q}}(\bar{x}), \end{aligned} \quad (25)$$

$$\begin{aligned} \bar{\boldsymbol{\zeta}}(\bar{x}, z) &= \begin{bmatrix} \zeta_{xxx}(\bar{x}, z) \\ \zeta_{zxx}(\bar{x}, z) \\ 2\zeta_{xxz}(\bar{x}, z) \end{bmatrix} = \mathbf{P}_2(z) \bar{\mathbf{H}}\bar{\mathbf{q}}(\bar{x}), \\ \delta \bar{\boldsymbol{\zeta}}(\bar{x}, z) &= \mathbf{P}_2(z) \bar{\mathbf{H}}\delta \bar{\mathbf{q}}(\bar{x}), \end{aligned} \quad (26)$$

$$\bar{\mathbf{q}}(\bar{x}) = [u(\bar{x}) \quad w(\bar{x}) \quad \psi(\bar{x})]^T,$$

$$\bar{\mathbf{E}} = \mathbf{E} | \partial/\partial x \rightarrow \partial/\partial \bar{x},$$

$$\bar{\mathbf{H}} = \mathbf{H} | \partial/\partial x \rightarrow \partial/\partial \bar{x}. \quad (27)$$

$$\bar{\mathbf{S}}(\bar{x}, z) = \int_x k(|x - \bar{x}|, \kappa) \mathbf{A} \mathbf{e}(x, z) dx, \quad \bar{\mathbf{T}}(\bar{x}, z) = \int_x k(|x - \bar{x}|, \kappa) \hat{\mathbf{A}} \boldsymbol{\zeta}(x, z) dx, \quad (18)$$

$$\bar{\mathbf{S}}(\bar{x}, z) = \begin{bmatrix} S_{xx}(\bar{x}, z) \\ S_{xz}(\bar{x}, z) \end{bmatrix}, \quad \bar{\mathbf{T}}(\bar{x}, z) = \begin{bmatrix} T_{xxx}(\bar{x}, z) \\ T_{zxx}(\bar{x}, z) \\ T_{xxz}(\bar{x}, z) \end{bmatrix}, \quad (19)$$

$$\mathbf{A} = \begin{bmatrix} \lambda + 2\mu & 0 \\ 0 & k_s \mu \end{bmatrix}, \quad \hat{\mathbf{A}} = \begin{bmatrix} 2(a_1 + a_2 + a_3 + a_4 + a_5) & 0 & 0 \\ 0 & 2(a_2 + a_4) & \frac{1}{2}(a_1 + 2a_5) \\ 0 & \frac{1}{2}(a_1 + 2a_5) & \frac{1}{2}(a_3 + 2a_4 + a_5) \end{bmatrix}. \quad (20)$$

Box I

Via performing the following analytical integrations:

$$\mathbf{C} = \int_A \mathbf{P}_1^T \mathbf{A} \mathbf{P}_1 dA, \quad \hat{\mathbf{C}} = \int_A \mathbf{P}_2^T \hat{\mathbf{A}} \mathbf{P}_2 dA, \quad (28)$$

one arrives at:

$$W = \frac{1}{2} \int_{\bar{x}} \left( \bar{\mathbf{q}}^T \bar{\mathbf{E}}^T \int_x k \mathbf{C} \mathbf{E} \mathbf{q} dx + \bar{\mathbf{q}}^T \bar{\mathbf{H}}^T \int_x k \hat{\mathbf{C}} \mathbf{H} \mathbf{q} dx \right) d\bar{x}, \quad (29)$$

$$\delta W = \int_{\bar{x}} \left( \delta \bar{\mathbf{q}}^T \bar{\mathbf{E}}^T \int_x k \mathbf{C} \mathbf{E} \mathbf{q} dx + \delta \bar{\mathbf{q}}^T \bar{\mathbf{H}}^T \int_x k \hat{\mathbf{C}} \mathbf{H} \mathbf{q} dx \right) d\bar{x}. \quad (30)$$

Besides, the kinetic energy is determined in the following manner:

$$T = \frac{1}{2} \int_V \rho \dot{u}_i(\bar{x}) \dot{u}_i(\bar{x}) dV, \quad (31)$$

where  $\rho$  signals the mass density of beam. From the following matrix-vector form of representation:

$$\bar{\mathbf{u}} = \mathbf{p} \bar{\mathbf{q}}, \quad \bar{\mathbf{u}}(\bar{x}, z) = [u_1(\bar{x}, z) \quad u_3(\bar{x}, z)]^T, \quad (32)$$

the kinetic energy and its variation are obtained as:

$$T = \frac{1}{2} \int_A \int_{\bar{x}} \rho \bar{\mathbf{u}}^T \bar{\mathbf{u}} d\bar{x} dA = \frac{1}{2} \int_{\bar{x}} \bar{\mathbf{q}}^T \rho \bar{\mathbf{q}} d\bar{x}, \quad (33)$$

$$\int_{t_1}^{t_2} \delta T dt = - \int_{t_1}^{t_2} \int_{\bar{x}} \delta \bar{\mathbf{q}}^T \rho \bar{\mathbf{q}} d\bar{x} dt, \quad (34)$$

in which:

$$\rho = \rho \int_A \mathbf{p}^T \mathbf{p} dA. \quad (35)$$

## 2.2. Differential nonlocal strain gradient model

According to the differential model of Eringen's nonlocal elasticity theory [11], the differential counterparts of Eqs. (8) and (9) are given by:

$$(1 - \kappa^2 \nabla^2) S_{ij} = \lambda \delta_{ij} e_{kk} + 2\mu e_{ij} = A_{ijkl} e_{kl}, \quad (36)$$

$$\begin{aligned} (1 - \kappa^2 \nabla^2) T_{ijk} &= \frac{1}{2} a_1 (\delta_{ij} \zeta_{kl} + 2\delta_{jk} \zeta_{li} + \delta_{ik} \zeta_{jl}) \\ &\quad + 2a_2 \delta_{jk} \zeta_{il} + a_3 (\delta_{ij} \zeta_{lk} + \delta_{ik} \zeta_{lj}) \\ &\quad + 2a_4 \zeta_{ijk} + a_5 (\zeta_{jki} + \zeta_{kji}) \\ &= \hat{A}_{ijklmn} \zeta_{lmn}, \end{aligned} \quad (37)$$

where the 1D Laplacian operator is  $\nabla^2 = \partial^2 / \partial x^2$ .

The matrix-vector form of Eqs. (36) and (37) is written as:

$$(1 - \kappa^2 \nabla^2) \mathbf{S} = \mathbf{A} \mathbf{e}, \quad (1 - \kappa^2 \nabla^2) \mathbf{T} = \hat{\mathbf{A}} \boldsymbol{\zeta}, \quad (38)$$

in which:

$$\mathbf{S} = [S_{xx} \quad S_{xz}]^T, \quad \mathbf{T} = [T_{xxx} \quad T_{zxx} \quad T_{xxz}]^T. \quad (39)$$

From Subsection 2.1, the vectors  $\mathbf{e}$ ,  $\boldsymbol{\zeta}$  and matrices  $\mathbf{A}$ ,  $\hat{\mathbf{A}}$  in Eqs. (15) and (20), respectively, can also be found.

For the strain energy one has:

$$W = \frac{1}{2} \int_A \int_x (S_{ij} e_{ij} + T_{ijk} \zeta_{ijk}) dx dA, \quad (40)$$

or:

$$\begin{aligned}
W &= \frac{1}{2} \int_A \int_x \left( \mathbf{e}^T \mathbf{S} + \boldsymbol{\zeta}^T \mathbf{T} \right) dx dA \\
&= \frac{1}{2} \int_A \int_x \left( \mathbf{q}^T \mathbf{E}^T \mathbf{P}_1^T \mathbf{S} + \mathbf{q}^T \mathbf{H}^T \mathbf{P}_2^T \mathbf{T} \right) dx dA \\
&= \frac{1}{2} \int_x \mathbf{q}^T \left( \mathbf{E}^T \mathbf{s} + \mathbf{H}^T \mathbf{t} \right) dx, \quad (41)
\end{aligned}$$

where  $\mathbf{s}$  and  $\mathbf{t}$  denote the classical and strain gradient resultant vectors, respectively, given as:

$$\mathbf{s} = \int_A \mathbf{P}_1^T \mathbf{S} dA, \quad (1 - \kappa^2 \nabla^2) \mathbf{s} = \mathbf{C} \mathbf{E} \mathbf{q}, \quad (42)$$

$$\mathbf{t} = \int_A \mathbf{P}_2^T \mathbf{T} dA, \quad (1 - \kappa^2 \nabla^2) \mathbf{t} = \hat{\mathbf{C}} \mathbf{H} \mathbf{q}, \quad (43)$$

in which  $\mathbf{C}$  and  $\hat{\mathbf{C}}$  are presented in Eq. (28). Therefore, in the differential model, the variation of strain energy is achieved as follows:

$$\delta W = \int_x \delta \mathbf{q}^T \left( \mathbf{E}^T \mathbf{s} + \mathbf{H}^T \mathbf{t} \right) dx. \quad (44)$$

Now, considering:

$$\begin{aligned}
T &= \frac{1}{2} \int_x \dot{\mathbf{q}}^T \boldsymbol{\rho} \dot{\mathbf{q}} dx, \\
\int_{t_1}^{t_2} \delta T dt &= - \int_{t_1}^{t_2} \int_x \delta \mathbf{q}^T \boldsymbol{\rho} \mathbf{q} dx dt. \quad (45)
\end{aligned}$$

and using Hamilton's principle lead to:

$$\begin{aligned}
&\int_{t_1}^{t_2} \int_x \delta \mathbf{q}^T \left( \mathbf{E}^T \mathbf{s} + \mathbf{H}^T \mathbf{t} + \boldsymbol{\rho} \mathbf{q} \right) dx dt \\
&= \int_{t_1}^{t_2} \int_x \delta \mathbf{q}^T \left( \left( \mathbf{E}^T \mathbf{C} \mathbf{E} + \mathbf{H}^T \hat{\mathbf{C}} \mathbf{H} \right) \mathbf{q} \right. \\
&\quad \left. + \boldsymbol{\rho} (1 - \kappa^2 \nabla^2) \mathbf{q} \right) dx dt = 0. \quad (46)
\end{aligned}$$

Regarding Eq. (46), the variations of equivalent strain and kinetic energies are obtained as:

$$\int_{t_1}^{t_2} \delta W dt = \int_{t_1}^{t_2} \int_x \delta \mathbf{q}^T \left( \mathbf{E}^T \mathbf{C} \mathbf{E} + \mathbf{H}^T \hat{\mathbf{C}} \mathbf{H} \right) \mathbf{q} dx dt, \quad (47)$$

$$\int_{t_1}^{t_2} \delta T dt = - \int_{t_1}^{t_2} \int_x \delta \mathbf{q}^T \boldsymbol{\rho} (1 - \kappa^2 \nabla^2) \mathbf{q} dx dt. \quad (48)$$

### 3. IGA

IGA is used in this work for the solution procedure. Using IGA has several advantages: In this type of analysis, through suitable solution properties such as generating unified geometry in a patch and implementing efficient refinement approaches, the difficulty of significant run time does not exist. Moreover, an important advantage of using IGA for a nonlocal strain gradient model is that the order of basis functions can be increased and gradients in SGT can be obtained in this approach readily. Hence, in contrast to FEM, there is no need to use Hermite functions.

#### 3.1. Integral nonlocal strain gradient model

For this model, to perform IGA, it is required that a novel solution procedure be developed. In other words, at any given point of  $\bar{x}$ , the assemblage of stress vectors should be performed in the entire domain of  $x$ . Then, by the outer assemblage in  $\bar{x}$  domain, the total stiffness matrix is obtained. In a patch, the displacement components of beam are interpolated by appropriate shape functions. The corresponding local coordinates of  $x$  and  $\bar{x}$  domains are indicated by  $\xi$  and  $\bar{\xi}$ , respectively. Considering NURBS basis function of  $i$ th knot as  $N_i$ , one has:

$$\begin{aligned}
\mathbf{q} &= \mathbf{N}(\xi) \mathbf{d}, \quad \mathbf{N}(\xi) = \mathbf{I}_3 \otimes \hat{\mathbf{N}}(\xi), \\
\hat{\mathbf{N}}(\xi) &= [N_1(\xi) \quad \dots \quad N_n(\xi)], \quad (49)
\end{aligned}$$

$$\begin{aligned}
\bar{\mathbf{q}} &= \bar{\mathbf{N}}(\bar{\xi}) \bar{\mathbf{d}}, \quad \bar{\mathbf{N}}(\bar{\xi}) = \mathbf{I}_3 \otimes \hat{\mathbf{N}}(\bar{\xi}), \\
\hat{\mathbf{N}}(\bar{\xi}) &= [N_1(\bar{\xi}) \quad \dots \quad N_n(\bar{\xi})], \quad (50)
\end{aligned}$$

where  $\mathbf{d}$  and  $\bar{\mathbf{d}}$  are the control variables in  $\xi$ - and  $\bar{\xi}$ -coordinates, respectively. Furthermore,  $\otimes$  is the Kronecker product and  $\mathbf{I}_p$  denotes the  $p$ -by- $p$  identity matrix.

Thus, the strain and strain gradient vectors and their variations are determined in a typical patch as:

$$\begin{aligned}
\mathbf{e}(\xi) &= \mathbf{P}_1 \mathbf{B}(\xi) \mathbf{d}, \quad \bar{\mathbf{e}}(\bar{\xi}) = \mathbf{P}_1 \bar{\mathbf{B}}(\bar{\xi}) \bar{\mathbf{d}}, \\
\delta \bar{\mathbf{e}}(\bar{\xi}) &= \mathbf{P}_1 \bar{\mathbf{B}}(\bar{\xi}) \delta \bar{\mathbf{d}}, \quad (51)
\end{aligned}$$

$$\begin{aligned}
\boldsymbol{\zeta}(\xi) &= \mathbf{P}_2 \mathbf{D}(\xi) \mathbf{d}, \quad \bar{\boldsymbol{\zeta}}(\bar{\xi}) = \mathbf{P}_2 \bar{\mathbf{D}}(\bar{\xi}) \bar{\mathbf{d}}, \\
\delta \bar{\boldsymbol{\zeta}}(\bar{\xi}) &= \mathbf{P}_2 \bar{\mathbf{D}}(\bar{\xi}) \delta \bar{\mathbf{d}}, \quad (52)
\end{aligned}$$

where:

$$\mathbf{B}(\xi) = \mathbf{E} \mathbf{N}(\xi), \quad \bar{\mathbf{B}}(\bar{\xi}) = \bar{\mathbf{E}} \bar{\mathbf{N}}(\bar{\xi}), \quad (53)$$

$$\mathbf{D}(\xi) = \mathbf{H} \mathbf{N}(\xi), \quad \bar{\mathbf{D}}(\bar{\xi}) = \bar{\mathbf{H}} \bar{\mathbf{N}}(\bar{\xi}). \quad (54)$$

The following relations are used in order to obtain the

stress vectors corresponding to the classical and strain gradient theories:

$$\mathbf{M} = \mathbf{R}\mathbf{d}, \quad \hat{\mathbf{M}} = \hat{\mathbf{R}}\mathbf{d}, \quad (55)$$

$$\mathbf{R} = \int_{\xi} k\mathbf{C}\mathbf{B}Jd\xi, \quad \hat{\mathbf{R}} = \int_{\xi} k\hat{\mathbf{C}}\mathbf{D}Jd\xi, \quad (56)$$

in which  $J$  is the determinant of Jacobian transformation matrix. By performing the inner assemblage process in  $\xi$ -coordinate, one can denote the total matrices of  $\mathbf{R}$ ,  $\hat{\mathbf{R}}$ , and vector  $d$  by  $\mathbb{R}$ ,  $\hat{\mathbb{R}}$ , and  $\mathbf{d}$ , respectively. Accordingly, the strain energy of the patch and its variation are determined as:

$$W_e = \frac{1}{2} \int_{\bar{\xi}} \left( \bar{\mathbf{d}}^T \bar{\mathbf{B}}^T \mathbb{R} \mathbf{d} + \bar{\mathbf{d}}^T \bar{\mathbf{D}}^T \hat{\mathbb{R}} \mathbf{d} \right) \bar{J} d\bar{\xi}, \quad (57)$$

$$\delta W_e = \int_{\bar{\xi}} \delta \bar{\mathbf{d}}^T \left( \bar{\mathbf{B}}^T \mathbb{R} + \bar{\mathbf{D}}^T \hat{\mathbb{R}} \right) \mathbf{d} \bar{J} d\bar{\xi} = \delta \bar{\mathbf{d}}^T \mathbf{K}_{s,p} \mathbf{d}, \quad (58)$$

where  $\bar{J}$  is the counterpart of  $J$  in  $\bar{\xi}$ -coordinates. The secant stiffness matrix of the patch,  $\mathbf{K}_{s,p}$ , is achieved as:

$$\mathbf{K}_{s,p} = \int_{\bar{\xi}} \left( \bar{\mathbf{B}}^T \mathbb{R} + \bar{\mathbf{D}}^T \hat{\mathbb{R}} \right) \bar{J} d\bar{\xi}. \quad (59)$$

In addition, the variation of kinetic energy of the patch can be expressed as:

$$\int_{t_1}^{t_2} \delta T_p dt = - \int_{t_1}^{t_2} \delta \bar{\mathbf{d}}^T \mathbf{M}_p \bar{\mathbf{d}} dt, \quad (60)$$

here  $\mathbf{M}_p$  stands for the inertia matrix given by:

$$\mathbf{M}_p = \int_{\bar{\xi}} \bar{\mathbf{N}}^T \rho \bar{\mathbf{N}} \bar{J} d\bar{\xi}. \quad (61)$$

By assembling the stiffness and inertia matrices, the total matrices and vectors of  $\mathbb{K}_s$ ,  $\mathbb{M}$ , and  $\bar{\mathbf{d}}$  are obtained. If one chooses the same local coordinate for  $\xi$  and  $\bar{\xi}$ , one finds that  $\mathbf{d} = \bar{\mathbf{d}}$ . Hence:

$$\int_{t_1}^{t_2} \delta W dt = \int_{t_1}^{t_2} \delta \mathbf{d}^T \mathbb{K}_s \mathbf{d} dt, \quad (62)$$

$$\int_{t_1}^{t_2} \delta T dt = - \int_{t_1}^{t_2} \delta \mathbf{d}^T \mathbb{M} \mathbf{d} dt. \quad (63)$$

Finally, using Hamilton's principle results in:

$$\mathbb{M} \mathbf{d} + \mathbb{K}_s \mathbf{d} = 0. \quad (64)$$

### 3.2. Differential nonlocal strain gradient model

For the differential nonlocal strain gradient model, the conventional assemblage process of IGA is performed. Thus, one has:

$$\mathbf{q} = \mathbf{N} \mathbf{d}, \quad \mathbf{N} = \mathbf{I}_3 \otimes \hat{\mathbf{N}}, \quad \hat{\mathbf{N}} = [N_1 \quad \dots \quad N_n], \quad (65)$$

$$\mathbf{e} = \mathbf{P}_1 \mathbf{B} \mathbf{d}, \quad \boldsymbol{\zeta} = \mathbf{P}_2 \mathbf{D} \mathbf{d}, \quad (66)$$

$$\mathbf{B} = \mathbf{E} \mathbf{N}, \quad \mathbf{D} = \mathbf{H} \mathbf{N}. \quad (67)$$

By inserting the presented interpolation into the equivalent energies in Eqs. (47) and (48), the variations of strain energy and kinetic energy are found as:

$$\int_{t_1}^{t_2} \delta W_p dt = \int_{t_1}^{t_2} \delta \mathbf{d}^T \mathbf{K}_{s,p} \mathbf{d} dt, \quad (68)$$

$$\int_{t_1}^{t_2} \delta T_p dt = - \int_{t_1}^{t_2} \delta \mathbf{d}^T \mathbf{M}_p \mathbf{d} dt, \quad (69)$$

where the stiffness and inertia matrices of the patch are expressed as:

$$\mathbf{K}_{s,p} = \int_{\xi} \left( \mathbf{B}^T \mathbf{C} \mathbf{B} + \mathbf{D}^T \hat{\mathbf{C}} \mathbf{D} \right) J d\xi, \quad (70)$$

$$\mathbf{M}_p = \int_{\xi} \mathbf{N}^T \rho (1 - \kappa^2 \nabla^2) \mathbf{N} J d\xi. \quad (71)$$

At last, by finding total matrices and vectors, the equations of motion are derived as Eq. (64).

## 4. Results and discussion

In this section, selected numerical results are presented to simultaneously analyze the effects of nonlocal and strain gradient parameters on the free vibration response of small-scale beams under clamped-free, pinned-pinned, and clamped-pinned end conditions. The results are generated for both integral nonlocal strain gradient and differential nonlocal strain gradient models. The following effective material and geometrical properties are considered:

$$\nu = 0.35, \quad k_s = 5/6, \quad L/h = 15.$$

The non-dimensional frequency is introduced as:

$$\Omega = \omega L \sqrt{\rho / (\lambda + 2\mu)}.$$

Also, the standard kernel function is used as:

$$k(|x - \bar{x}|, \kappa) = \frac{1}{2\kappa} e^{-\frac{|x - \bar{x}|}{\kappa}}.$$

First, some comparisons are made to examine the integrity of the present formulation as well as to verify the proposed solution approach. Initially, the advantages of using IGA in the nonlocal strain gradient theory are clarified. As expressed in Section 3, according to the piecewise continuous polynomials basis functions in the standard NURBS-based IGA, the consistency of deformation gradients has been satisfied in the entire domain of the patch. However, Hermite shape functions and additional Degrees Of Freedom (DOFs) should be considered in the finite element analysis of stain gradient theory. In this regard, Table 1 is provided to compare the first three frequencies of pinned and clamped beams determined by the present isogeometric analysis and finite element analysis of [69]. The results are produced by using the classical, modified couple stress, and modified strain gradient theories in different thickness-to-length scale ratios. Ansari et al. [69] employed 3-node beam element with Hermite

shape functions including four DOFs at each node ( $w, \psi, w', \psi'$ ). The excellent agreement of results in Table 1 shows the efficiency of the present standard IGA models of nonlocal strain gradient elasticity.

Also, it would be interesting to compare the outcome of the present size-dependent theory with the Molecular Dynamics (MD) simulations. Due to the confirmed accuracy of MD analysis of small-scale structures, one can calibrate the nonlocal and length scale parameters through such comparison. To this end, Ref. [70] is considered and single-walled carbon nanotubes are modelled via the present size-dependent Timoshenko beam theory. According to the integral nonlocal modified strain gradient theory, different combinations of nonlocal and length scale parameters can be found, which produce the same results of MD. For instance, two sets of  $(\kappa, l)$  are shown in Figure 1 at which, corresponding to clamped-free and clamped-clamped end conditions, the frequencies

**Table 1.** Comparison of the first three frequencies of pinned-pinned and clamped-clamped nano-beams versus the non-dimensional small-scale parameter based on different strain gradient theories.

$\frac{h}{l}$	Theory	Present (IGA)			Ref. [69] (FEA)		
		1st mode	2nd mode	3rd mode	1st mode	2nd mode	3rd mode
Pinned-pinned							
1	CT	1.6379	6.2015	12.9054	1.6379	6.2015	12.9054
	MCST	2.9660	11.0772	22.7934	2.9661	11.0772	22.7934
	MSGT	4.4269	14.1670	26.9350	4.4269	14.1670	26.9351
5	CT	0.3276	1.2403	2.5811	0.3276	1.2403	2.5811
	MCST	0.3424	1.2969	2.7008	0.3424	1.2969	2.7008
	MSGT	0.3756	1.4054	2.8868	0.3757	1.4055	2.8868
10	CT	0.1638	0.6202	1.2905	0.1638	0.6202	1.2905
	MCST	0.1657	0.6274	1.3058	0.1657	0.6274	1.3058
	MSGT	0.1702	0.6424	1.3323	0.1702	0.6424	1.3324
20	CT	0.0819	0.3101	0.6453	0.0819	0.3101	0.6453
	MCST	0.0821	0.3110	0.6472	0.0821	0.3110	0.6472
	MSGT	0.0827	0.3129	0.6506	0.0828	0.3129	0.6506
Clamped-clamped							
1	CT	3.4810	8.7805	15.6511	3.4810	8.7805	15.6511
	MCST	6.2225	15.5963	27.8798	6.2225	15.5963	27.8798
	MSGT	8.2014	18.9531	33.4258	8.2014	18.9531	33.4259
5	CT	0.6962	1.7561	3.1302	0.6962	1.7561	3.1302
	MCST	0.7298	1.8491	3.3138	0.7298	1.8491	3.3138
	MSGT	0.8199	2.0304	3.5756	0.8199	2.0305	3.5756
10	CT	0.3481	0.8781	1.5651	0.3481	0.8781	1.5651
	MCST	0.3529	0.8929	1.5975	0.3529	0.8929	1.5975
	MSGT	0.3718	0.9318	1.6531	0.3718	0.9319	1.6531
20	CT	0.1741	0.4390	0.7826	0.1741	0.4390	0.7826
	MCST	0.1749	0.4424	0.7910	0.1749	0.4424	0.7911
	MSGT	0.1804	0.4538	0.8068	0.1804	0.4538	0.8068



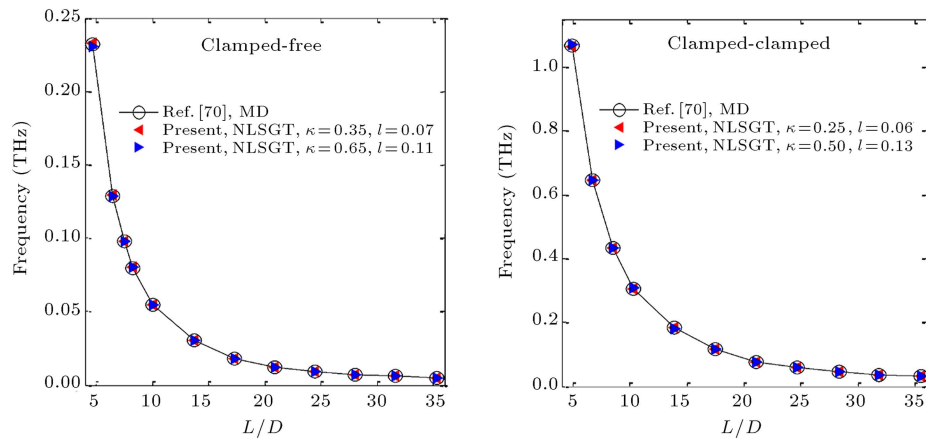


**Figure 1.** Fundamental frequencies of clamped-free and clamped-clamped nanotubes versus the length-to-diameter ratio based on MD simulations [70] and the present integral nonlocal modified strain gradient model.

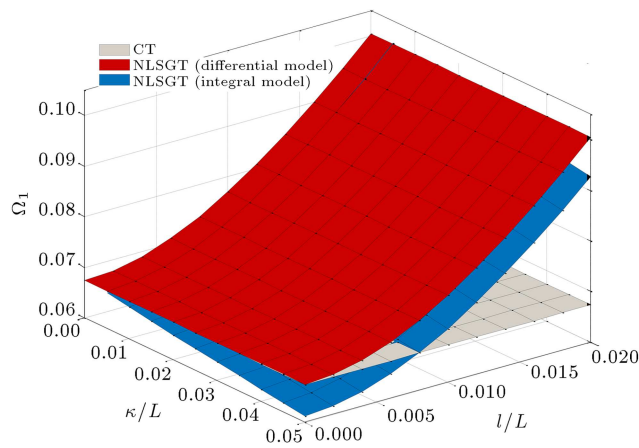


**Figure 2.** Variation of non-dimensional fundamental frequency of clamped-free nano-beam versus the non-dimensional small-scale and nonlocal parameters based on differential and integral model of nonlocal modified strain gradient theory.

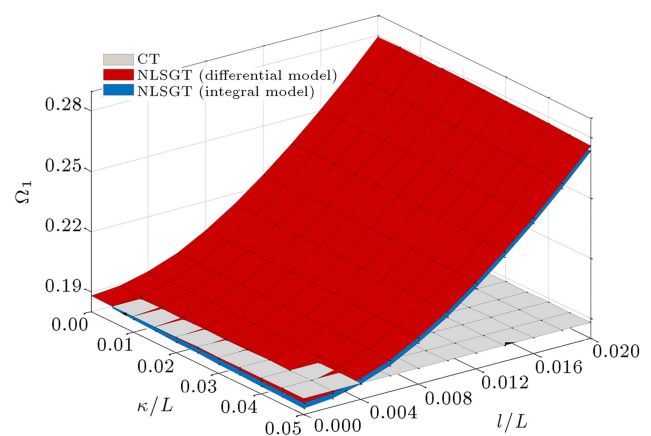


**Figure 3.** Variation of non-dimensional fundamental frequency of pinned-pinned nano-beam versus the non-dimensional small-scale and nonlocal parameters based on differential and integral model of nonlocal modified strain gradient theory.

of NLSGT perfectly match the ones of molecular dynamics.

In Figures 2-4, the first dimensionless natural frequency of beams is plotted against dimensionless nonlocal and small-scale parameters corresponding to clamped-free, pinned-pinned, and clamped-pinned boundary conditions, respectively. The dimensionless nonlocal parameter is defined as nonlocal parameter-to-length ratio ( $\kappa/l$ ), and dimensionless small scale parameter is defined as material length scale parameter-to-length ratio ( $l/L$ ). The results of these figures are generated based on two models: integral nonlocal strain gradient and differential nonlocal strain gradient models. Also, the results from the classical elasticity theory (CT) are presented for the comparison purpose. Additionally, the strain gradient model is based on the modified strain gradient theory with the assumption of  $l_0 = l_1 = l_2 = l$ . The effects of length scale and nonlocal parameters can be studied here simultane-

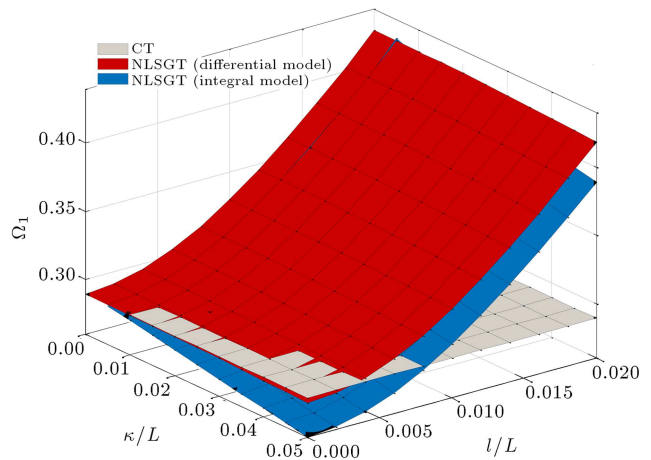


**Figure 4.** Variation of non-dimensional fundamental frequency of clamped-pinned nano-beam versus the non-dimensional small-scale and nonlocal parameters based on differential and integral model of nonlocal modified strain gradient theory.

ously. It is first observed that the strain gradient effect is more pronounced than nonlocality effect. Increasing the length scale parameter leads to the increase in frequency for all types of boundary conditions. Whereas, the nonlocal effect on the free vibrations of beams is dependent on the selected model. In the case of cantilever, the frequency slightly increases by increasing the dimensionless nonlocal parameter based on the differential nonlocal model, while the frequency decreases as  $\kappa/L$  gets larger based on the integral nonlocal model. For other boundary conditions, increasing the nonlocal parameter has a decreasing influence on the frequency of structure based on both models. However, the decrease in frequency using the integral model is more prominent than that based on the differential model, especially for clamped-pinned beam. It can also be found that there are some specific values of nonlocal and length scale parameters at which the predictions of integral nonlocal strain gradient model become identical to those of the classical model.

Figures 5-7 show the variations of the first and second natural frequencies of beams with the dimensionless nonlocal parameter according to five models. These models are the classical model, differential nonlocal model (Diff. NL), integral nonlocal model (Int. NL), differential nonlocal modified strain gradient model (Diff. NLSGT), and integral nonlocal modified strain gradient model (Int. NLSGT). Figures 5-7 are given for clamped-free, pinned-pinned, and clamped-pinned beams, respectively. Figure 5 reveals that based on the differential nonlocal model (and differential nonlocal modified strain gradient model), the first

natural frequency of clamped-free beam increases with increase in nonlocal parameter, which is a paradox. Such a paradox is not observed for the second mode of vibration as reported in [71]. In contrast, increasing the nonlocal parameter has a decreasing effect on the natural frequencies of cantilever based on the integral nonlocal model (and integral nonlocal modified strain gradient model). It should be noted that the decrease in second frequency based on the integral model is more pronounced than that based on the differential model. Also, Figures 6 and 7 indicate that using the differential nonlocal model does not lead to paradoxical results for pinned-pinned and clamped-pinned beams. As can be expected, the combined nonlocal strain gradient models predict the vibration frequencies larger than their nonlocal counterparts do due to the stiffening effects of strain gradient terms. The results also show that at a given value of  $\kappa/L$ , the smallest frequency belongs to the integral nonlocal model and the largest one is computed based upon the differential nonlocal modified strain gradient model.

In Figures 8-10, the first frequency of beams with different boundary conditions is plotted versus the dimensionless small-scale parameter based on various strain gradient models including the modified couple stress model (MCST), Aifantis's strain gradient model (SGT), the modified strain gradient model (MSGT), and their combinations with the integral nonlocal model. It is seen that based on all models, the frequency increases as  $l/L$  becomes larger. It is also observed that the difference between the results of models tends to diminish with decreasing the dimensionless

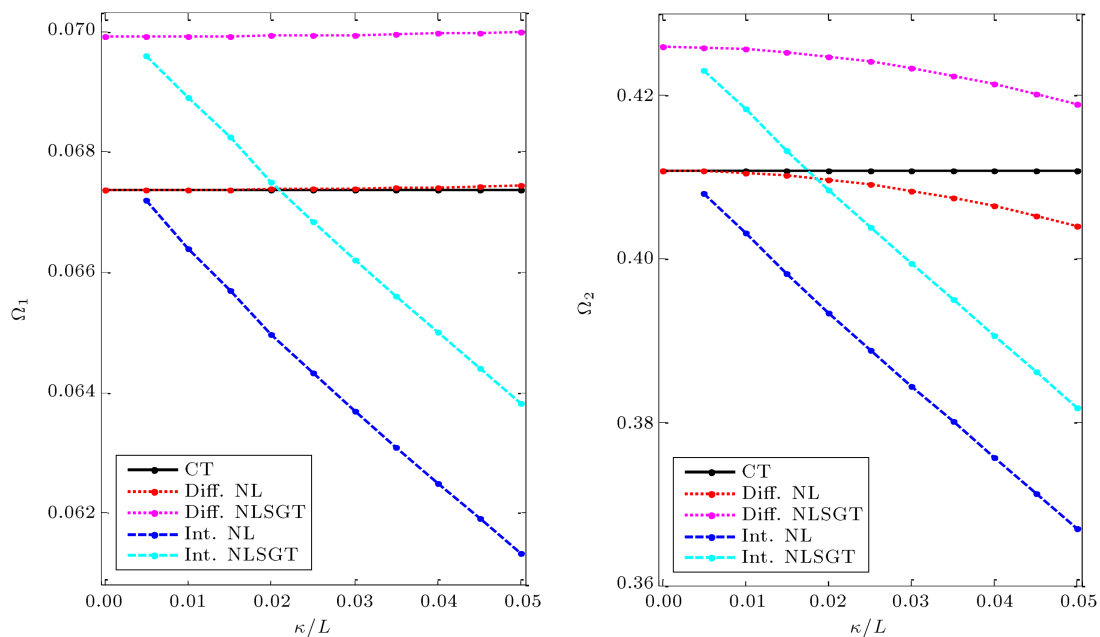


**Figure 5.** Variations of non-dimensional frequencies of the 1st and 2nd modes of clamped-free nano-beam versus the non-dimensional nonlocal parameter based on differential and integral model of nonlocal continuum and corresponding nonlocal modified strain gradient theory ( $l/L = 0.005$ ).

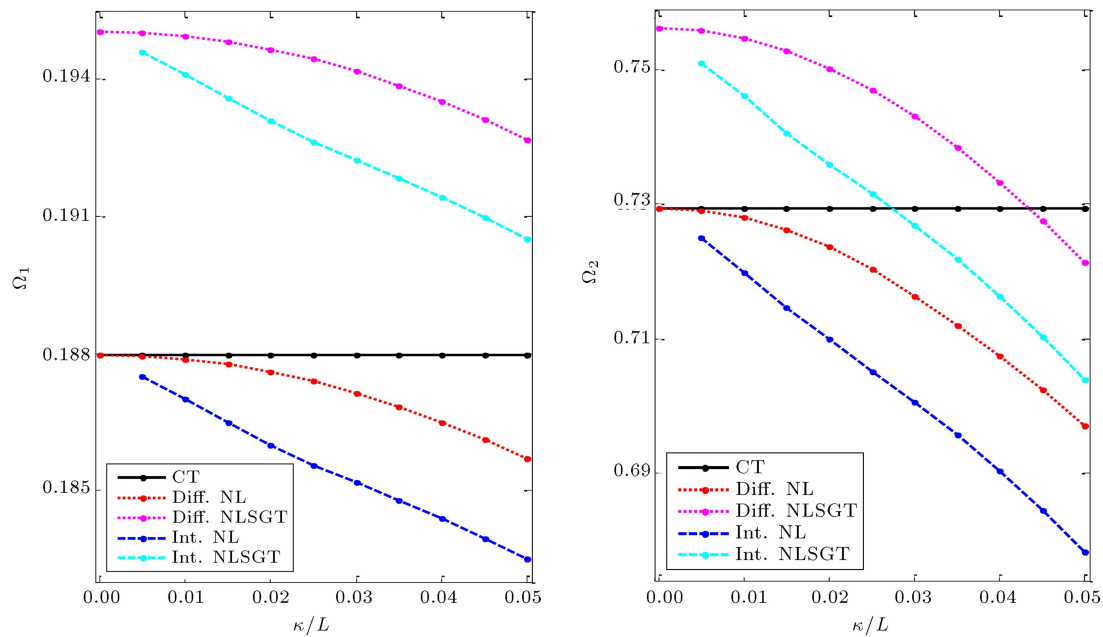


**Figure 6.** Variations of non-dimensional frequencies of the 1st and 2nd modes of pinned-pinned nano-beam versus the non-dimensional nonlocal parameter based on differential and integral model of nonlocal continuum and corresponding nonlocal modified strain gradient theory ( $l/L = 0.005$ ).

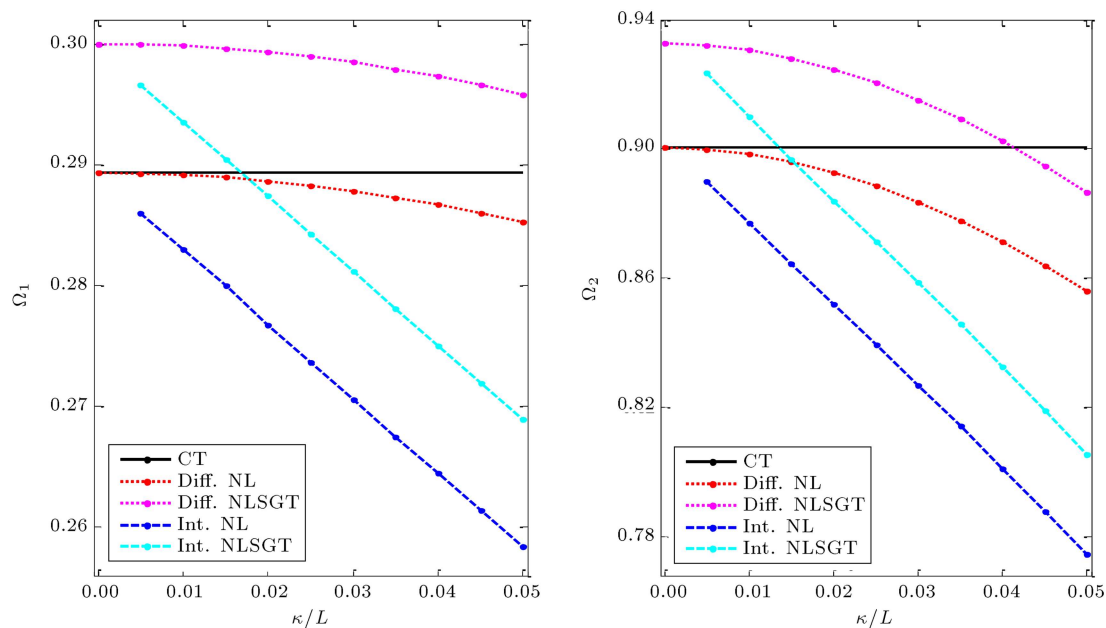


**Figure 7.** Variations of non-dimensional frequencies of the 1st and 2nd modes of clamped-pinned nano-beam versus the non-dimensional nonlocal parameter based on differential and integral model of nonlocal continuum and corresponding nonlocal modified strain gradient theory ( $l/L = 0.005$ ).

small-scale parameter. Another finding is that the stiffening effect of strain gradient terms is the highest based on the modified strain gradient theory and is the lowest based on the modified couple stress theory. Furthermore, integral nonlocal strain gradient models can have underestimation or overestimation compared to the classical theory depending on the value of length scale parameter.

## 5. Conclusion

In this article, the vibrational characteristics of small-scale Timoshenko beams were studied based on the nonlocal strain gradient theory. To accomplish this goal, Eringen's nonlocal theory in conjunction with the most general strain gradient theory was utilized. The beam model was formulated according to both

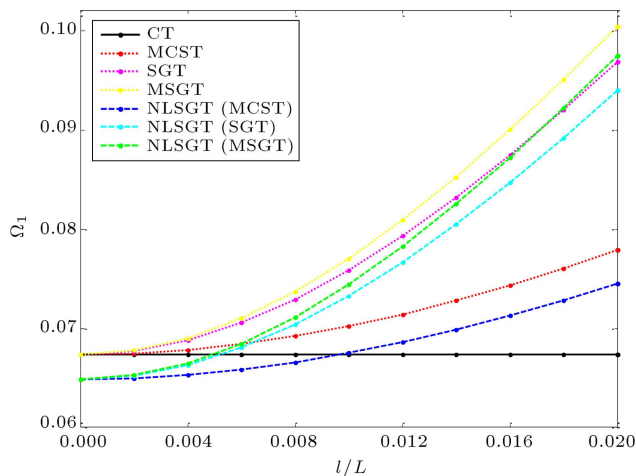


**Figure 8.** Variation of non-dimensional fundamental frequency of clamped-free nano-beam versus the non-dimensional small-scale parameter based on strain gradient theories and corresponding integral model of nonlocal strain gradient theories ( $\kappa/L = 0.02$ ).

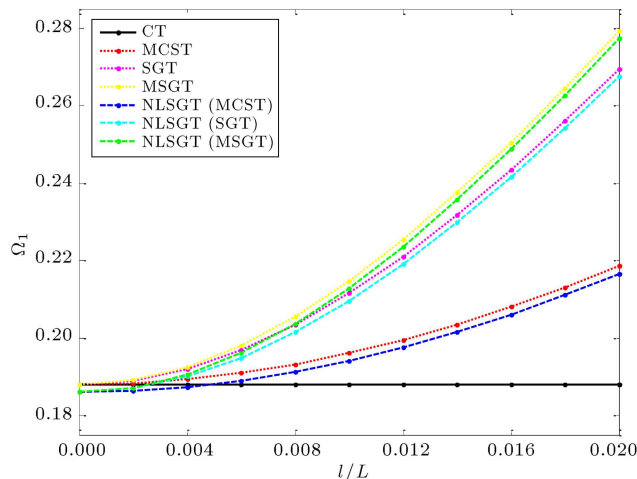


**Figure 9.** Variation of non-dimensional fundamental frequency of pinned-pinned nano-beam versus the non-dimensional small-scale parameter based on strain gradient theories and corresponding integral model of nonlocal strain gradient theories ( $\kappa/L = 0.02$ ).

original (integral) and differential forms of nonlocal theory. Also, the adopted strain gradient theory was the most general one with additional non-classical material constants used for capturing small-scale effects. Hamilton's principle was used in order to obtain the governing equations of motion. Moreover, the governing equations were derived in the vector-matrix form, which could be readily employed in the finite element or isogeometric analyses. IGA was then applied for the solution procedure. The effects of nonlocal parameter of nonlocal theory and length scale parameter of strain gradient theories on the frequencies of pinned-pinned, clamped-free, and clamped-pinned nano-beams were investigated in detail. In addition, comparisons were

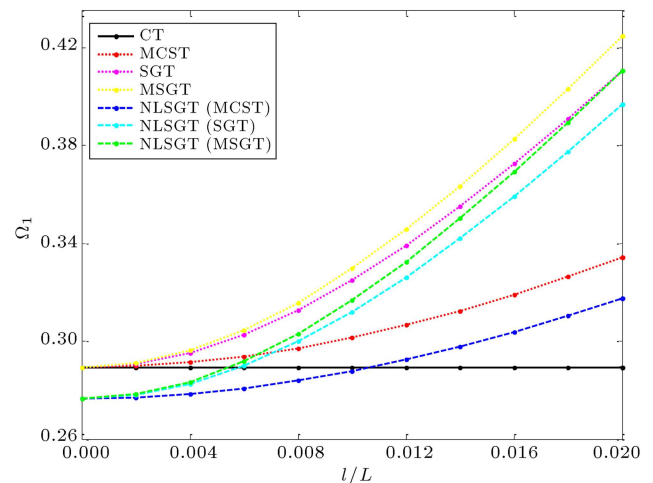


**Figure 10.** Variation of non-dimensional fundamental frequency of clamped-pinned nano-beam versus the non-dimensional small-scale parameter based on strain gradient theories and corresponding integral model of nonlocal strain gradient theories ( $\kappa/L = 0.02$ ).

made between the predictions of differential/integral nonlocal models, strain gradient models, and nonlocal strain gradient models. Some important findings of the study can be summarized as follows:

- The strain gradient influence is more prominent than the nonlocal effect. Also, by the increase in length scale parameter, beams under all kinds of boundary conditions vibrate with larger frequencies. The nonlocal effect in the differential model is dependent on the selected end conditions and vibration mode;
- Using the differential nonlocal model to calculate the fundamental frequencies of cantilevers leads to paradoxical results and recourse must be made to the integral formulation of Eringen's nonlocal theory. Such a paradox does not exist at higher modes and for other boundary conditions;
- The smallest and largest frequencies are obtained based upon the integral nonlocal model and the differential nonlocal modified strain gradient model, respectively. Furthermore, comparison between different strain gradient models reveals that the stiffening effect of strain gradient terms is the highest according to the modified strain gradient theory and is the lowest based upon the modified couple stress theory;
- The nonlocal and strain gradient effects cancel each other out for some specific values of nonlocal and length scale parameters;
- The standard NURBS-based IGA provides the consistency of higher gradients in different types of strain gradient and nonlocal - strain gradient theories. This leads to achieving more efficient solution

strategy than the finite element analysis, which requires Hermite shape functions and additional DOFs;

- With appropriate set of size-dependent material constants, the integral nonlocal modified strain gradient theory matches the molecular dynamics simulation.

## References

1. Ansari, R., Norouzzadeh, A., Shakouri, A., Bazdid-Vahdati, M., and Rouhi, H. "Finite element analysis of vibrating microbeams/microplates using a three-dimensional micropolar element", *Thin-Walled Struct.*, **124**, pp. 489-500 (2018).
2. Tadi Beni, Y., Mehralian, F., and Zeighampour, H. "The modified couple stress functionally graded cylindrical thin shell formulation", *Mech. Adv. Mat. Struct.*, **23**, pp. 791-801 (2016).
3. Ansari, R., Norouzzadeh, A., Gholami, R., Faghieh Shojaei, M., and Darabi, M.A. "Geometrically nonlinear free vibration and instability of fluid-conveying nanoscale pipes including surface stress effects", *Microfluidics Nanofluidics*, **20**, pp. 1-14 (2016).
4. Akgöz, B. and Civalek, Ö. "Bending analysis of embedded carbon nanotubes resting on an elastic foundation using strain gradient theory", *Acta Astronautica*, **119**, pp. 1-12 (2016).
5. Mehralian, F. and Tadi Beni, Y. "Size-dependent torsional buckling analysis of functionally graded cylindrical shell", *Compos. Part B: Eng.*, **94**, pp. 11-25 (2016).
6. Kröner, E. "Elasticity theory of materials with long range cohesive forces", *Int. J. Solids Struct.*, **3**, pp. 731-742 (1967).
7. Krumhansl, J. "Some considerations of the relation between solid state physics and generalized continuum mechanics", In E. Kröner (Ed.), *Mechanics of generalized Continua, IUTAM symposia*, Springer Berlin Heidelberg, pp. 298-311 (1968).
8. Kunin, I.A. "The theory of elastic media with microstructure and the theory of dislocations", In E. Kröner (Ed.), *Mechanics of generalized Continua, IUTAM symposia*, Springer Berlin, Heidelberg, pp. 321-329 (1968).
9. Eringen, A.C. "Nonlocal polar elastic continua", *Int. J. Eng. Sci.*, **10**, pp. 1-16 (1972).
10. Eringen, A.C. and Edelen, D.G.B. "On nonlocal elasticity", *Int. J. Eng. Sci.*, **10**, pp. 233-248 (1972).
11. Eringen, A.C. "On differential equations of nonlocal elasticity and solutions of screw dislocation and surface waves", *J. Appl. Phys.*, **54**, pp. 4703-4710 (1983).
12. Ansari, R., Shahabodini, A., and Rouhi, H. "A non-local plate model incorporating interatomic potentials for vibrations of graphene with arbitrary edge conditions", *Curr. Appl. Phys.*, **15**, pp. 1062-1069 (2015).
13. Shen, H.S., Shen, L., and Zhang, C.L. "Nonlocal plate model for nonlinear bending of single-layer graphene sheets subjected to transverse loads in thermal environments", *Appl. Phys. A*, **103**, pp. 103-112 (2011).
14. Ansari, R., Faghieh Shojaei, M., Shahabodini, A., and Bazdid-Vahdati, M. "Three-dimensional bending and vibration analysis of functionally graded nanoplates by a novel differential quadrature-based approach", *Compos. Struct.*, **131**, pp. 753-764 (2015).
15. Lu, P., Zhang, P.Q., Lee, H.P., Wang, C.M., and Reddy, J.N. "Non-local elastic plate theories", *Proc. Royal. Soc. A*, **463** (2007). DOI: 10.1098/rspa.2007.1903
16. Ansari, R. and Rouhi, H. "Explicit analytical expressions for the critical buckling stresses in a monolayer graphene sheet based on nonlocal elasticity", *Solid State Commun.*, **152**, pp. 56-59 (2012).
17. Ansari, R. and Norouzzadeh, A. "Nonlocal and surface effects on the buckling behavior of functionally graded nanoplates: An isogeometric analysis", *Physica E*, **84**, pp. 84-97 (2016).
18. Nguyen, N.T., Hui, D., Lee, J., and Nguyen-Xuan, H. "An efficient computational approach for size-dependent analysis of functionally graded nanoplates", *Comput. Meth. Appl. Mech. Eng.*, **297**, pp. 191-218 (2015).
19. Norouzzadeh, A. and Ansari, R. "Isogeometric vibration analysis of functionally graded nanoplates with the consideration of nonlocal and surface effects", *Thin-Walled Struct.* (In Press).
20. Wang, C.M., Zhang, H., Challamel, N., and Duan, W.H. "On boundary conditions for buckling and vibration of nonlocal beams", *Eur. J. Mech. - A/Solids*, **61**, pp. 73-81 (2017).
21. Ansari, R., Gholami, R., and Rouhi, H. "Size-dependent nonlinear forced vibration analysis of magneto-electro-thermo-elastic timoshenko nano-beams based upon the nonlocal elasticity theory", *Compos. Struct.*, **126**, pp. 216-226 (2015).
22. Yan, J.W., Tong, L.H., Li, C., Zhu, Y., and Wang, Z.W. "Exact solutions of bending deflections for nanobeams and nano-plates based on nonlocal elasticity theory", *Compos. Struct.*, **125**, pp. 304-313 (2015).
23. Ansari, R., Ramezannezhad, H., and Gholami, R. "Nonlocal beam theory for nonlinear vibrations of embedded multiwalled carbon nanotubes in thermal environment", *Nonlinear Dynam.*, **67**, pp. 2241-2254 (2012).
24. Ansari, R., Gholami, R., Sahmani, S., Norouzzadeh, A., and Bazdid-Vahdati, M. "Dynamic stability analysis of embedded multi-walled carbon nanotubes in thermal environment", *Acta Mechanica Solida Sinica*, **28**, pp. 659-667 (2015).
25. Sedighi, H.M., Keivani, M., and Abadyan, M. "Modified continuum model for stability analysis of asymmetric FGM double-sided NEMS: corrections due to finite conductivity, surface energy and nonlocal effect", *Compos. Part B: Eng.*, **83**, pp. 117-133 (2015).

26. Civalek, Ö. and Demir, C. “A simple mathematical model of microtubules surrounded by an elastic matrix by nonlocal finite element method”, *Appl. Math. Comput.*, **289**, pp. 335-352 (2016).
27. Rouhi, H. and Ansari, R. “Nonlocal analytical Flugge shell model for axial buckling of double-walled carbon nanotubes with different end conditions”, *NANO*, **7**, 1250018 (2012).
28. Demir, Ç. and Civalek, Ö. “Torsional and longitudinal frequency and wave response of microtubules based on the nonlocal continuum and nonlocal discrete models”, *Appl. Math. Model.*, **37**, pp. 9355-9367 (2013).
29. Ansari, R., Rouhi, H., and Mirnezhad, M. “Stability analysis of boron nitride nanotubes via a combined continuum-atomistic model”, *Scientia Iranica*, **20**, pp. 2314-2322 (2013).
30. Natsuki, T., Matsuyama, N., and Ni, Q.Q. “Vibration analysis of carbon nanotube-based resonator using nonlocal elasticity theory”, *Appl. Phys. A*, **120**, pp. 1309-1313 (2015).
31. Ansari, R., Shahabodini, A., and Rouhi, H. “A thickness-independent nonlocal shell model for describing the stability behavior of carbon nanotubes under compression”, *Compos. Struct.*, **100**, pp. 323-331 (2013).
32. Arani, A.G. and Hashemian, M. “Surface stress effects on dynamic stability of double-walled boron nitride nanotubes conveying viscous fluid based on nonlocal shell theory”, *Scientia Iranica*, **20**, p. 2356 (2013).
33. Polizzotto, C. “Nonlocal elasticity and related variational principles”, *Int. J. Solids Struct.*, **38**, pp. 7359-7380 (2001).
34. Challamel, N. and Wang, C. “The small length scale effect for a non-local cantilever beam: a paradox solved”, *Nanotechnology*, **19**, p. 345703 (2008).
35. Challamel, N., Rakotomanana, L., and Le Marrec, L. “A dispersive wave equation using nonlocal elasticity”, *Comptes Rendus Mécanique*, **337**, pp. 591-595 (2009).
36. Khodabakhshi, P. and Reddy, J.N. “A unified integro-differential nonlocal model”, *Int. J. Eng. Sci.*, **95**, pp. 60-75 (2015).
37. Fernández-Sáez, J., Zaera, R., Loya, J., and Reddy, J.N. “Bending of Euler-Bernoulli beams using Eringen's integral formulation: A paradox resolved”, *Int. J. Eng. Sci.*, **99**, pp. 107-116 (2016).
38. Norouzzadeh, A. and Ansari, R. “Finite element analysis of nano-scale Timoshenko beams using the integral model of nonlocal elasticity”, *Physica E*, **88**, pp. 194-200 (2017).
39. Norouzzadeh, A., Ansari, R., and Rouhi, H. “Pre-buckling responses of Timoshenko nanobeams based on the integral and differential models of nonlocal elasticity: An isogeometric approach”, *Appl. Phys. A*, **123**, p. 330 (2017).
40. Mindlin, R.D. “Micro-structure in linear elasticity”, *Arch. Ration. Mech. Anal.*, **6**, pp. 51-78 (1964).
41. Mindlin, R.D. “Second gradient of strain and surface tension in linear elasticity”, *Int. J. Solids Struct.*, **1**, pp. 417-438 (1965).
42. Lam, D.C.C., Yang, F., Chong, A.C.M., Wang, J., and Tong, P. “Experiments and theory in strain gradient elasticity”, *J. Mech. Phys. Solids*, **51**, pp. 1477-1508 (2003).
43. Aifantis, E.C. “On the role of gradients in the localization of deformation and fracture”, *Int. J. Eng. Sci.*, **30**, pp. 1279-1299 (1992).
44. Yang, F., Chong, A.C.M., Lam, D.C.C., and Tong, P. “Couple stress based strain gradient theory for elasticity”, *Int. J. Solids Struct.*, **39**, pp. 2731-2743 (2002).
45. Akgoz, B. and Civalek, O. “Buckling analysis of linearly tapered micro-columns based on strain gradient elasticity”, *Struct. Eng. Mech.*, **48**, pp. 195-205 (2013).
46. Nateghi, A. and Salamat-talab, M. “Thermal effect on size dependent behavior of functionally graded microbeams based on modified couple stress theory”, *Compos. Struct.*, **96**, pp. 97-110 (2013).
47. Chen, W.J. and Li, X.P. “Size-dependent free vibration analysis of composite laminated Timoshenko beam based on new modified couple stress theory”, *Arch. Appl. Mech.*, **83**, pp. 431-444 (2013).
48. Ansari, R., Norouzzadeh, A., Gholami, R., Faghieh Shojaei, M., and Hosseinzadeh, M. “Size-dependent nonlinear vibration and instability of embedded fluid-conveying SWBNNTs in thermal environment”, *Physica E*, **61**, pp. 148-157 (2014).
49. Akgöz, B. and Civalek, Ö. “Bending analysis of FG microbeams resting on Winkler elastic foundation via strain gradient elasticity”, *Compos. Struct.*, **134**, pp. 294-301 (2015).
50. Zeighampour, H., Tadi Beni, Y., and Mehralian, F. “A shear deformable conical shell formulation in the framework of couple stress theory”, *Acta Mechanica*, **226**, pp. 2607-2629 (2015).
51. Sadeghi, H., Baghani, M., and Naghdabadi, R. “Strain gradient thermoelasticity of functionally graded cylinders”, *Scientia Iranica*, **21**, pp. 1415-1423 (2014).
52. Zeighampour, H. and Tadi Beni, Y. “A shear deformable cylindrical shell model based on couple stress theory”, *Arch. Appl. Mech.*, **85**, pp. 539-553 (2015).
53. Ansari, R., Gholami, R., Norouzzadeh, A., and Sahmani, S. “Size-dependent vibration and instability of fluid-conveying functionally graded microshells based on the modified couple stress theory”, *Microfluidics Nanofluidics*, **19**, pp. 509-522 (2015).
54. Tadi Beni, Y. “Size-dependent electromechanical bending, buckling, and free vibration analysis of functionally graded piezoelectric nanobeams”, *J. Intel. Mat. Syst. Struct.*, **27**, pp. 2199-2215 (2016).
55. Kanani, A., Koochi, A., Farahani, M., Rouhi, E., and Abadyan, M. “Modeling the size dependent pull-in instability of cantilever nano-switch immersed in

- ionic liquid electrolytes using strain gradient theory”, *Scientia Iranica*, **23**, pp. 976-989 (2016).
56. Tadi Beni, Y. “Size-dependent analysis of piezoelectric nanobeams including electro-mechanical coupling”, *Mech. Res. Commun.*, **75**, pp. 67-80 (2016).
  57. Ansari, R., Gholami, R., and Norouzzadeh, A. “Size-dependent thermo-mechanical vibration and instability of conveying fluid functionally graded nanoshells based on Mindlin’s strain gradient theory”, *Thin-Walled Struct.*, **105**, pp. 172-184 (2016).
  58. Hadjesfandiari, A.R. and Dargush, G.F. “Couple stress theory for solids”, *Int. J. Solids Struct.*, **48**, pp. 2496-2510 (2011).
  59. Narendar, S. and Gopalakrishnan, S. “Ultrasonic wave characteristics of nanorods via nonlocal strain gradient models”, *J. Appl. Phys.*, **107**, 084312 (2010).
  60. Polizzotto, C. “A unifying variational framework for stress gradient and strain gradient elasticity theories”, *Eur. J. Mech. A/Solids*, **49**, pp. 430-440 (2015).
  61. Li, L., Hu, Y., and Ling, L. “Flexural wave propagation in small-scaled functionally graded beams via a nonlocal strain gradient theory”, *Compos. Struct.*, **133**, pp. 1079-1092 (2015).
  62. Farajpour, M.R., Rastgoo, A., Farajpour, A., and Mohammadi, M. “Vibration of piezoelectric nanofilm-based electromechanical sensors via higher-order nonlocal strain gradient theory”, *IET Micro & Nano Lett.*, **11**, pp. 302-307 (2016).
  63. Ebrahimi, F. and Barati, M.R. “Nonlocal strain gradient theory for damping vibration analysis of viscoelastic inhomogeneous nano-scale beams embedded in visco-Pasternak foundation”, *J. Vib. Control*, **24**, pp. 2080-2095 (2018).
  64. Mehralian, F., Tadi Beni, Y., and Karimi Zeverdejani, M. “Nonlocal strain gradient theory calibration using molecular dynamics simulation based on small scale vibration of nanotubes”, *Physica B*, **514**, pp. 61-69 (2017).
  65. Ebrahimi, F. and Barati, M.R. “Vibration analysis of viscoelastic inhomogeneous nanobeams resting on a viscoelastic foundation based on nonlocal strain gradient theory incorporating surface and thermal effects”, *Acta Mechanica*, **228**, pp. 1197-1210 (2017).
  66. Hughes, T.J., Cottrell, J.A., and Bazilevs, Y. “Isogeometric analysis: CAD, finite elements, NURBS, exact geometry and mesh refinement”, *Comput. Meth. Appl. Mech. Eng.*, **194**, pp. 4135-4195 (2005).
  67. Cottrell, J.A., Hughes, T.J., and Bazilevs, Y., *Isogeometric Analysis: Toward Integration of CAD and FEA*, John Wiley & Sons (2009).
  68. Park, S. and Gao, X. “Bernoulli-Euler beam model based on a modified couple stress theory, journal of micromechanics and microengineering”, *Journal of Micromechanics and Microengineering*, **16**, pp. 2355-2359 (2006).
  69. Ansari, R., Faghih Shojaei, M., and Rouhi, H., “Small-scale Timoshenko beam element”, *Euro. J. Mech. A/Solids*, **53**, pp. 19-33 (2015).
  70. Zhang, Y., Wang, C., and Tan, V. “Assessment of Timoshenko beam models for vibrational behavior of single-walled carbon nanotubes using molecular dynamics”, *Adv. Appl. Math. Mech.*, **1**, pp. 89-106 (2009).
  71. Challamel, N., Zhang, Z., Wang, C.M., Reddy, J.N., Wang, Q., Michelitsch, T., and Collet, B. “On non-conservativeness of Eringen’s nonlocal elasticity in beam mechanics: correction from a discrete-based approach”, *Arc. Appl. Mech.*, **84**, pp. 1275-1292 (2014).

## Biographies

**Amir Norouzzadeh** received his BSc and MSc degrees in Automotive and Mechanical Engineering, in 2012 and 2014, from Iran University of Science and Technology and University of Guilan, Iran, respectively. He is currently a PhD candidate in Mechanical Engineering at the University of Guilan, Iran. His research interests include computational mechanics, generalized continuum mechanics, finite element, and isogeometric analysis.

**Reza Ansari** received his PhD degree, in 2008, from the University of Guilan, Iran, where he is currently faculty member in the Department of Mechanical Engineering. He was also a visiting fellow at Wollongong University, Australia, during 2006-2007. He has authored numerous refereed journal papers and book chapters. His research interests include computational nano- and micro-mechanics, advanced numerical techniques, nonlinear analyses, and prediction of the mechanical behavior of smart composite/FGM shell-type structures.

**Hessam Rouhi** received his PhD degree in Mechanical Engineering, in 2016, from the University of Guilan, Iran. He is currently Faculty Member in the Department of Engineering Science, Faculty of Technology and Engineering, East of Guilan, University of Guilan, Iran. His research interests include computational micro- and nano-mechanics and the mechanical behavior of structures, including buckling and vibration.